

Cloudnet: Evaluation of model clouds using ground-based observations

R. J. Hogan^{*1}, A. J. Illingworth¹, E. J. O'Connor¹, D. Bouniol², M. E. Brooks³, J. Delanoë¹,
D. P. Donovan⁴, J. D. Eastment⁵, N. Gaussiat³, J. W. F. Goddard⁵, M. Haeffelin⁶,
H. Klein Baltink⁴, O. A. Krasnov⁷, J. Pelon², J.-M. Piriou⁸, A. Protat², H. W. J. Russchenberg⁷,
A. Seifert⁹, A. M. Tompkins¹⁰, G.-J. van Zadelhoff⁴, F. Vinit⁸, C. D. Westbrook¹, U. Willén¹¹,
D. R. Wilson³ and C. L. Wrench⁵

ABSTRACT

The Cloudnet project aims to provide a systematic evaluation of clouds in forecast and climate models by comparing the model output with continuous ground-based observations of the vertical profiles of cloud properties. Cloud profiles derived from cloud radars, lidars and dual-frequency microwave radiometers operated at three sites in France, the Netherlands and the United Kingdom for several years have been compared with the clouds in seven European forecast models. The advantage of this continuous appraisal is that robust and objective statistics are obtained on the performance of each model, as opposed to the limited information that is obtained when a single model is evaluated at one site during an unrepresentative case study. The variables evaluated in this paper are cloud fraction, liquid water content, ice water content and stratocumulus drizzle rate. The forecasts are evaluated using comparison of means and PDFs, and using skill scores. The Cloudnet analysis scheme is currently being expanded to include sites outside Europe.

1. Introduction

The effort to improve clouds in forecast models has been hampered by the difficulty of making accurate observations. In situ aircraft measurements reveal the macroscopic structure and typical water contents of clouds and the habits of ice crystals (e.g. Korolev *et al.*, 2000), but suffer from sampling problems, providing 1D cloud ‘snapshots’. Projects such as Cliwa-net (Crewell *et al.*, 2004) combined aircraft and ground based instrumentation to provide a more complete view. This was accomplished for a number of isolated case studies, raising the question of how typical the observed periods were. Remote sensing from space provides global cloud properties of cloud cover (Rossow and Schiffer; 1991; Webb *et al.*, 2001; Jakob, 2003), liquid water path (Greenwald *et al.*, 1993), and recently even information concerning ice water content has been derived from microwave limb sounding instruments (Li *et al.*, 2005). But satellite remotely sensed products have had the drawback that information concerning vertical structure is usually lacking; the recent successful launch of a cloud radar on CloudSat (Stephens *et al.*, 2002) accompanied by the Calipso lidar (Winker *et al.*, 2003) should provide extremely valuable information. The Cloudnet approach for evaluation of clouds in forecast models could be adopted for these new satellites. Cloudnet and the ongoing Atmospheric Radiation Measurement (ARM) project (Stokes and Schwartz, 1994) bridge the gap between the ground-based case studies and satellite remote sensing by operating a network of ground stations to continuously monitor cloud-related variables over multi-year time periods.

^{*}Corresponding author address: Robin J. Hogan, Department of Meteorology, University of Reading, Earley Gate, PO Box 243, Reading RG6 6BB, UK. Email: r.j.hogan@reading.ac.uk.

Affiliations:

¹Department of Meteorology, University of Reading, UK.

²Institute Pierre Simon Laplace, Centre d’Etudes des Environnements Terrestres et Planétaires, Velizy, France.

³Met Office, Exeter, UK.

⁴Royal Netherlands Meteorological Institute, De Bilt, The Netherlands.

⁵CCLRC-Rutherford Appleton Laboratory, Didcot, UK.

⁶Institute Pierre Simon Laplace, LMD, France.

⁷Delft University of Technology, IRCTR, Delft, The Netherlands.

⁸Météo France, Toulouse, France.

⁹Deutscher Wetterdienst, Offenbach, Germany.

¹⁰European Centre for Medium-Range Weather Forecasts, Reading, UK.

¹¹Swedish Meteorological and Hydrological Institute, Norrköping, Sweden.

One dilemma commonly highlighted is the difficulty of converting knowledge gained from cloud observations into global and specific model improvements. Often, model modifications that address biases observed in case studies do not translate into general improvements in forecast skill. Moreover, in-depth analysis of complex field studies hinders quasi-realtime feedback for modellers; unfortunate, since most numerical weather prediction models are under continual development and feedback not pertaining to the most recent model cycle is awkward to interpret and frequently discarded. In addition, model developers are often unaware of the details of observational retrieval techniques (such as signal attenuation, rainfall contamination, and so on) rendering direct model-observation inter-comparisons unreliable. Finally, continuous data sets of observed cloud-related variables can be used to suggest new physically based parameterisation schemes which can be tested off-line and their performance quantified before operational implementation.

In order to address these issues, Cloudnet set out to directly involve a number of European operational forecast centres in a cooperative effort to evaluate and improve their skill in cloud predictions (see Table 1 for details of the centres involved). The goal was to establish a number of ground-based remote sensing sites, which would all be equipped with a specific array of instrumentation, using active sensors such as lidar and Dopplerized mm-wave radar, in order to provide vertical profiles of the main cloud variables (cloud fraction, ice and liquid water contents), at high spatial and temporal resolution, and equivalently for all sites involved. Following the ethos of the ARM project, these sites have operated continuously for a multi-year period in order to gain statistics unaffected by seasonality. However, by establishing the participation of the modelling centres, Cloudnet was able to uniquely develop robust algorithms for processing model output to precisely simulate the retrieved cloud information. Part of the success of Cloudnet was to establish a framework in which this could be provided in quasi-realtime, in order to always provide up-to-date monitoring of the latest operational cycle of the numerical weather prediction models. Figure 1 shows the location of the Cloudnet sites (now including Lindenberg) and ARM sites worldwide. This paper includes work described by Illingworth *et al.* (2007) and O'Connor *et al.* (2007). Real time observations and model forecasts, together with daily and monthly quicklooks and statistics of model performance can be found on the Cloudnet web site <http://www.cloud-net.org/>.

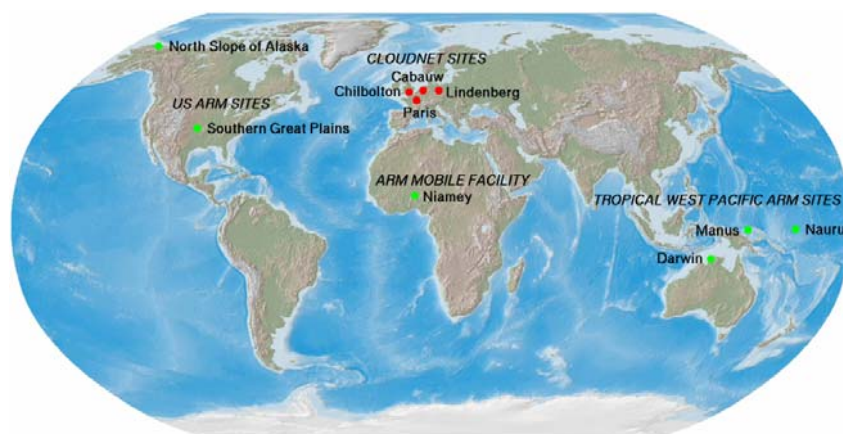


Figure 1. Continuously operating cloud observatories worldwide (in 2006 when the ARM Mobile Facility was located at Niamey). Each is equipped with a large suite of active and passive remote sensing instruments, plus standard met instruments. The observations at Cabauw were augmented with 3-GHz radar measurements for better IWC. Palaiseau observations included a cloud-aerosol depolarisation lidar (Haefelin *et al.*, 2005). The Chilbolton 3-GHz radar provided calibration for all other radars in Cloudnet. The ARM sites were described by Stokes and Schwartz (1994).

Table 1. Summary of the characteristics of each of the seven models evaluated in Cloudnet. Cloudnet involved six modelling centres. It is emphasized that these operational models are under evolution in terms of their physics, data assimilation methods and resolution, and the table provides some indications of the main versions included in the Cloudnet analysis period. RACMO and RCA are regional climate models without data assimilation.

Institute	Model	Horizontal res. (km)	Vertical levels	Forecast range (hrs)	Cloud scheme
ECMWF	ECMWF Integrated Forecast System	39	60	12-35	Tiedtke (1993): prognostic cloud fraction and total water; diagnostic liquid/ice ratio.
Met Office	Unified Model (UM): mesoscale	12	38	6-11	Wilson and Ballard (1999): diagnostic cloud fraction (Smith 1990); prognostic vapour+liquid and ice mixing ratios.
Met Office	UM: global	60	38	0-21	As Met Office mesoscale model.
Météo France	ARPEGE	24	41	12-35	Diagnostic water content, sub-grid convection (Ducrocq and Bougeault, 1995). Cloud fraction: Xu and Randall (1996).
Royal Netherlands Meteorological Institute (KNMI)	Regional Atmospheric Climate Model (RACMO)	18	40	12-36	As ECMWF model. Boundary conditions from ECMWF forecasts.
Swedish Meteorological and Hydrological Institute (SMHI)	Rosby Centre Regional Atmospheric Model (RCA)	44	24	1-24*	Diagnostic cloud fraction (Rasch and Kristjánsson, 1998), prognostic total water with diagnostic liquid/ice ratio. *Hindcasts, using ECMWF analyses at model boundaries
Deutscher Wetterdienst (DWD)	Lokal Modell (LM)	7	35	6-17	Doms et al. (2004): diagnostic cloud fraction, prognostic cloud water, cloud ice, snow and rain mixing ratios.

2. The Cloudnet data products

The procedure for deriving cloud properties from ground-based observations for evaluating models is not trivial. The fundamental variables to be tested are the fraction of the model gridbox containing cloud and the mass of liquid and ice condensate within each box. Each of the sites has a different mix of instruments so a crucial part of Cloudnet has been to devise a uniform set of procedures and data formats to enable the algorithms to be applied at all sites and used to test all models. The data products in the Cloudnet processing chain are summarized in Table 2. The “core” instruments used in cloud retrievals at each site are a Doppler cloud radar, a lidar ceilometer, a dual- or multi-wavelength microwave radiometer and a rain gauge, as described by Illingworth *et al.* (2007). All these instruments operate unattended 24 hours per day. Whilst superior performance is offered by a high-power lidar, fully automatic high-power lidar systems were not available for the Cloudnet project. However, an important use of the lidar is to identify the base of low-level water clouds that cannot be distinguished by radar, and a low-cost unattended lidar ceilometer is adequate for this purpose.

Table 2. Organization of Cloudnet products. The raw 1-s data recorded by the instruments are designated Level 0 and are not released as Cloudnet products but are available from the individual participants.

Level	Description	Example products
1a	Uncalibrated observations in NetCDF format with any instrumental artifacts removed	<ul style="list-style-type: none"> • Radar reflectivity factor and Doppler velocity • Lidar attenuated backscatter coefficient • Microwave radiometer brightness temperatures • Surface rain rate
1b	Calibrated data in NetCDF format	<ul style="list-style-type: none"> • Radar reflectivity factor and Doppler velocity • Lidar attenuated backscatter coefficient • Microwave radiometer liquid water path • Hourly model analyses and forecasts • Surface rain rate
1c	Observations on a common high-resolution grid with correction for radar attenuation, categorization of targets, error variables and data quality flags	<ul style="list-style-type: none"> • Instrument Synergy/Target Categorization
2a	Derived meteorological products at high resolution (typically 30 s and 60 m)	<ul style="list-style-type: none"> • Liquid water content • Ice water content • Drizzle flux and drizzle drop size from radar and lidar • Ice effective radius from radar and lidar • TKE dissipation rate from radar Doppler velocity
2b	Derived meteorological products averaged to the vertical and horizontal grid of each model, together with the model value for comparison	<ul style="list-style-type: none"> • Cloud fraction in each model gridbox • Gridbox-mean liquid water content • Gridbox-mean ice water content
3	Monthly and yearly statistics on the performance of each model	<ul style="list-style-type: none"> • Cloud fraction means, PDFs and skill scores • Liquid water content means, PDFs and skill scores • Ice water content means, PDFs and skill scores

The first step in the processing is to perform 30-s averaging of the raw observations from each site and then convert to NetCDF format using common conventions for the storage of metadata. These Level 1a datasets are then calibrated and stored as Level 1b products (see Table 2). Radar calibration has been achieved by comparison to the absolutely calibrated 3-GHz weather radar at Chilbolton (Goddard *et al.* 1994); during the project the mobile RASTA radar travelled between the three sites to ensure a consistent calibration between all radars. The resulting calibration was consistent with the 94-GHz radar calibration method of Hogan *et al.* (2003a). The traditional method for calibrating visible wavelength lidars is to monitor the level of the known Rayleigh backscatter from air molecules, but this does not work for ceilometers that typically operate at longer wavelengths of around 1 μm . We therefore use the method of O'Connor *et al.* (2004), which enables calibration to 10% whenever optically thick stratocumulus is overhead. A method (Gaussiat *et al.*, 2007) to improve the accuracy of liquid water path derived from dual-wavelength radiometers that has been shown to be reliable is to use the ceilometer to identify profiles free from liquid water and use these to effectively recalibrate the radiometer brightness temperatures, in a similar way to the technique of van Meijgaard and Crewell (2005).

2.1. Instrument synergy and target categorization

To facilitate the application of synergetic algorithms, the observations by the core instruments are then combined into a single Level 1c dataset where many of the necessary pre-processing tasks are performed. The observations are first averaged to a common grid (typically 30 s in time and 60 m in height); radar and lidar observations for a typical day over the ARM Southern Great Plains site are shown in the top two panels

of Figure 2. These are supplemented by temperature, pressure, humidity and wind speed from an operational model to assist with attenuation correction and cloud phase identification.

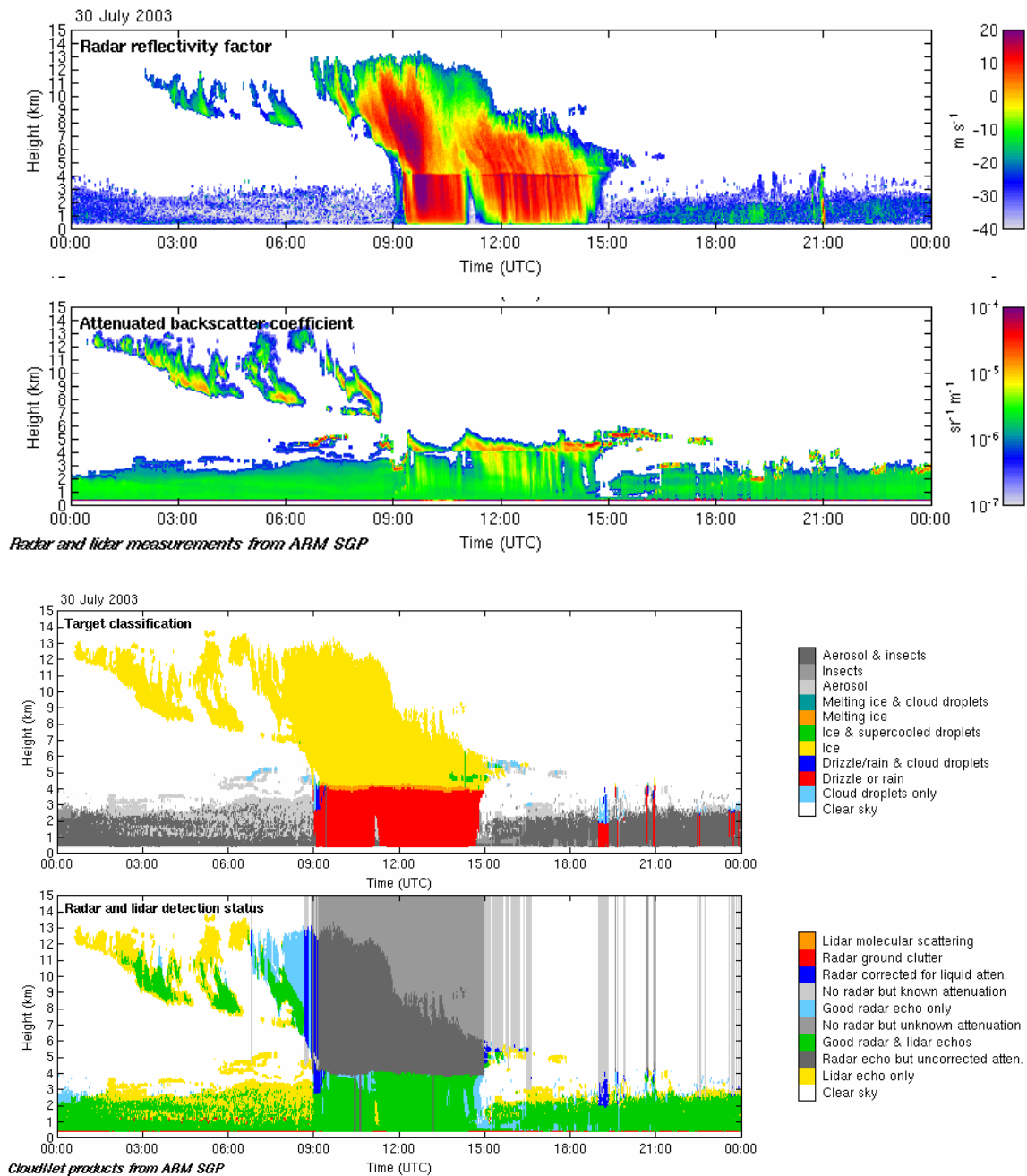


Figure 2. (Top two panels) One day's calibrated radar and lidar observations from the ARM SGP site on 30 July 2003. (Bottom two panels) An example of the corresponding classification of targets and data quality field of the Instrument Synergy/Target Categorization dataset of Table 2 (Hogan and O'Connor, 2004).

In order to know when one may apply a particular algorithm, the backscatter targets in each radar/lidar pixel are then categorized into a number of different classes as shown in third panel of Fig. 3. Full details of this procedure are given by Hogan and O'Connor (2004), but essentially we make use of the fact that radar is sensitive to large particles such as rain and drizzle drops, ice particles and insects, while the lidar is sensitive to higher concentrations of smaller particles such as cloud droplets and aerosol. The high lidar backscatter of liquid droplets enables supercooled liquid layers to be identified even when embedded within ice clouds

(Hogan *et al.* 2003b), while a step-change in vertical Doppler velocity in the vicinity of the 0°C line in the model temperature field indicates the presence of melting ice.

Radar reflectivity, Z , is then corrected for attenuation to ensure the accuracy of algorithms that make use of it. Water vapour and molecular oxygen attenuation is estimated using the thermodynamic variables from the model, but ensuring that the air is saturated when a cloud is observed by the radar or lidar. The two-way gaseous attenuation is typically 1-3 dB to cirrus altitudes at 94 GHz. Liquid water attenuation is calculated by estimating the profile of liquid water content using a combination of radiometer-derived liquid water path and the cloud base and top heights from radar and lidar, as described later. At 94 GHz the two-way attenuation due to a cloud with a liquid water path of 500 g m⁻² is around 4.5 dB. At 35 GHz the attenuation due to both liquid water and gases is substantially smaller. Attenuation correction is deemed unreliable when rainfall is observed at the ground and above melting ice because of uncertainties in the retrieved liquid water path, additional attenuation due to water on the radar instrument (Hogan *et al.* 2003a) and unknown attenuation by melting particles. A data quality field is therefore provided (lower panel of Fig. 3) to indicate the reliability of the radar and lidar data at each pixel.

Finally, variables are added to indicate the likely random and systematic error of each measured field, enabling the corresponding errors in the retrieved meteorological variables to be estimated. Additionally, a variable is added containing the minimum detectable Z as a function of height, enabling one to take account of the tenuous ice clouds that the radar is unable to detect when comparing observations with models (e.g. Hogan *et al.* 2001).

2.2. Meteorological products

The various Cloudnet algorithms are then applied to the Instrument Synergy/Target Categorization dataset. The first step is to derive liquid water content (LWC), ice water content (IWC) and other variables on the same high-resolution grid as the observations (designated Level 2a products in Table 2). Data is extracted from the model every hour to provide hourly snapshots over the Cloudnet sites. We follow the approach of previous workers (e.g. Mace *et al.* 1998, Hogan *et al.* 2001) and use temporal averaging to yield the equivalent of a two-dimensional slice through the three-dimensional model gridbox. Using the model wind speed as a function of height and the known horizontal model gridbox size, the appropriate averaging time may be calculated; for example, for the 39-km resolution of the ECMWF model, a 20 m s⁻¹ wind speed would correspond to a 33-min averaging time centred on the time of the model snapshot. It is assumed that in this time the cloud structure observed is predominantly due to the advection of structure within the gridbox across the site, rather than evolution of the cloud during the period. Nonetheless, the averaging time is constrained to lie between 10 and 60 mins, to ensure that a representative sample of data is used when the winds are very light or very strong. In a similar fashion, cloud fraction is estimated simply as the fraction of pixels within the two-dimensional slice that are categorized as either liquid, supercooled, or ice cloud. Hence for observations with a resolution of 30 s and 60 m, and a gridbox 180-m thick, cloud fraction would be derived from around 200 independent pixels. As each model has different horizontal and vertical resolutions, a separate Level 2b product is produced for each model. Finally, monthly and yearly statistics of model performance are calculated for each model and each variable as Level 3 datasets and displayed on the Cloudnet web site.

3. Evaluation of model cloud fraction

The large quantity of near-continuous data from the three Cloudnet sites enables us to make categorical statements about the cloud fraction climatology of each of the models, much more than was possible previously from limited and unrepresentative case studies. As described in the previous section, cloud fraction is calculated on the grid of each of the various models as a Level 2 product. For the purpose of this

study, we calculate cloud fraction by volume rather than by area (see Brooks *et al.*, 2005, for a detailed discussion). Following Hogan *et al.* (2001) we argue that there is a strong distinction between liquid cloud and liquid precipitation, but we treat cloud and precipitation as a continuum in the ice phase; certainly from remote and in situ observations there is no obvious distinction in terms of IWC or optical depth. This leads to falling ice being treated as a cloud but if these particles melt at the zero-degree level to form rain, they are then no longer classified as cloud. The same assumption is also made in the Met Office model (Wilson and Ballard 1999), but not in the other models, in which falling snow is separate from cloud and does not contribute to radiative transfer. Further discussion of this point was provided by Hogan *et al.* (2001), who showed that the mid-level ECMWF cloud fraction compared better to radar observations if falling snow above 0.05 mm hr^{-1} (melted-equivalent rate) in the model was added to the model cloud fraction. In this study we chose not to do this because such hydrometeors do not contribute to radiative transfer in the model and so cannot really be thought of as clouds. The sensitivity to high cloud can be diminished by strong radar attenuation in moderate and heavy rain, which would lead to an underestimate of cloud fraction in the observations. For sites with a 35-GHz radar, periods with a rain rate greater than 8 mm hr^{-1} are excluded from the comparison, while for sites with a 94-GHz radar (which suffers greater attenuation), the threshold is 2 mm hr^{-1} .

Full monthly and yearly comparisons are recorded and are available for each model/observatory on the Cloudnet web site. Figure 3 depicts both the mean cloud fraction versus height and the probability distribution function of the observations and the models, for a year of data at all three sites. Some substantial errors in the various models are evident, such as the large overestimate in boundary-layer cloud fraction in the KNMI RACMO and SMHI RCA models, and the difficulty both versions of the Met Office model have in simulating completely cloudy gridboxes. All but one of the models underestimate the mean fraction of mid-level cloud. For some models, better mid-level performance would be achieved by treating ice

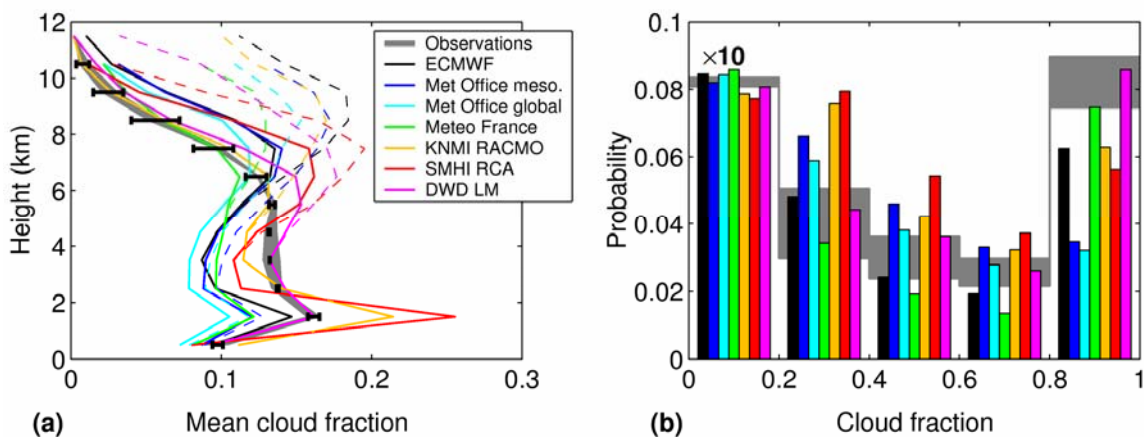


Figure 3. (a) Mean cloud fraction over Chilbolton, Palaiseau and Cabauw for 2004 from the observations and the seven models. The observations have been averaged to the periods for which each model was available, but as some models were not available for the full year the observed mean cloud fraction is slightly different, as indicated by the width of the observation line. Two lines are shown for each model: the thick solid lines show the model after filtering to remove ice clouds too tenuous for the radar to detect, while the thin dashed lines are for all model clouds. The error bars give an approximate indication of the uncertainties in the filtering procedure, calculated by changing the minimum-detectable radar reflectivity (estimated separately at each site as a function of time and height) by $\pm 3 \text{ dB}$. Although the error bars are shown only on the observations, they indicate the uncertainty in the comparison itself. (b) Corresponding histograms of observed and filtered-model cloud fraction for clouds below 7 km. Note that the bars between cloud fractions of 0 and 0.2 are shown at a tenth of their true height. The width of the gray observation line is due to the fact that the observed cloud fractions are calculated for different averaging times (due to the different model horizontal resolutions) and larger averaging times tend to lead to fewer completely full or empty gridboxes and more frequent partially filled gridboxes.

precipitation as cloud (Hogan *et al.* 2001), but the fact that the Met Office model (which does treat ice precipitation as cloud) also has a substantial underestimate indicates that this is a deeper problem associated with the poor representation of the phase of these clouds (e.g. Hogan *et al.* 2003b). Due to the problem of radar sampling of high clouds, care must be taken in judging model performance above 8 km; the solid lines in the figure show the model after filtering to remove ice clouds too tenuous for the radar to detect, while the dashed lines are for all model clouds although it has been demonstrated within Cloudnet that this problem can be overcome by the use of high power lidar (Protat *et al.* 2006).

3.1. Quantifying the effect of changing the cloud scheme on cloud fraction in the Météo-France and ECMWF models

Between 2003 and 2005 two major changes were introduced into the Météo-France cloud scheme that were designed and tuned to improve cloud radiative forcings and improve the capability of predicting winter cyclogenesis. Figure 4 depicts the cloud fraction from the model in April 2003, in which the sudden change in behaviour can be seen. Figure 5 shows a corresponding dramatic increase in cloud fraction, bringing the model much closer to the Cloudnet observations. However, the evaluation of cloud fraction versus human observations of total cloud cover at synoptic stations in France showed that in 2002 the total cloud cover in the model was essentially unbiased, but by 2005 it was systematically around 20% too *low*. At first glance it is difficult to reconcile the two contradictory sources of information, but one of the additional changes made to the model was to switch from a random overlap scheme to maximum-random overlap. Random overlap is known to result in a substantial overestimate of total cloud cover given a profile of cloud fraction values (e.g. Hogan and Illingworth, 2000), but it seems that before April 2003 the cloud fraction was underestimated to just the right extent that the total cloud cover was correct, on average. After this time, the increase in cloud fraction does not seem to have been enough to counter the reduction in total cloud cover associated with moving to a maximum-random overlap scheme. The current underestimate in total cloud cover evident in Fig. 5 is likely to be due to a combination of the residual underestimate in cloud fraction and the fact that radar observations have shown that the maximum-random assumption tends to somewhat underestimate total cloud cover (Hogan and Illingworth 2000, Mace and Benson-Troth 2002, Willén *et al.* 2005). This example shows just how misleading can be the use of total cloud cover alone, and the need to evaluate cloud fraction objectively as a function of height using radars and lidars, as well as to ensure that the correct overlap scheme is in use.

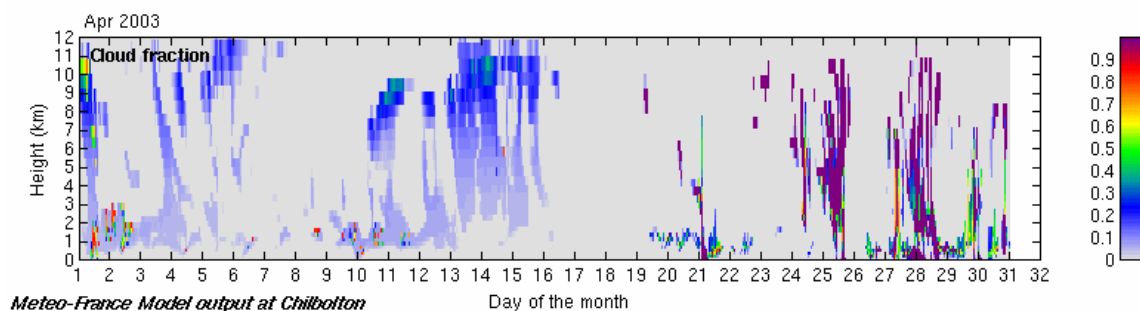


Figure 4. Cloud fraction versus height for the Météo-France model over Chilbolton in April 2003, demonstrating clearly the change in cloud scheme in the middle of the month.

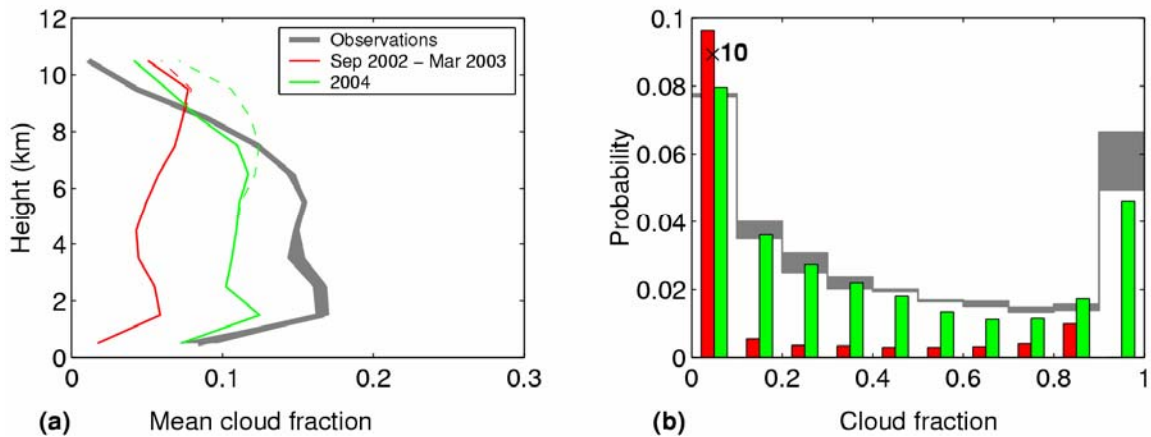


Figure 5. (a) As Fig. 3 but for the Météo-France model before and after a significant change in the cloud scheme in April 2003. The red line/bars correspond to comparisons at Cabauw before this date, while the green show the improved performance in 2004 averaged over all sites. Panel b shows histograms of cloud fraction between 0 and 3 km (with the bars for cloud fractions between 0 and 0.1 shown at a tenth of their true height).

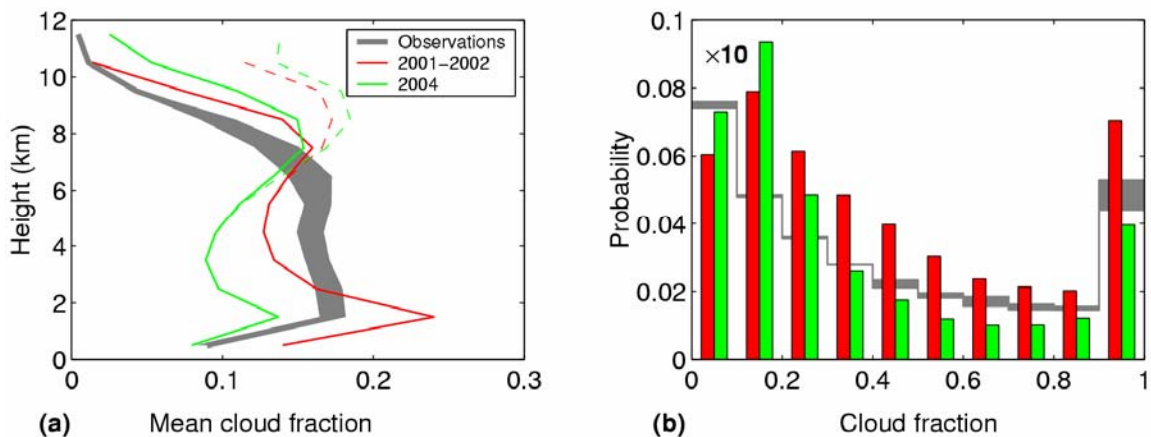


Figure 6. (a) As Figure 5 but for the ECMWF model before and after a significant change in the cloud scheme. The red line and bars corresponds to comparisons at Cabauw before this date, while the green lines show a comparison averaged over all sites for the year 2004.

The Cloudnet observations have also been used to evaluate changes in the ECMWF model cloud fraction scheme. Figure 6 shows that in 2001-2002 the ECMWF model was overestimating the mean boundary-layer cloud fraction by around 50%. Revisions to the model numerics, cloud scheme and convection scheme after this time have seemingly overcompensated for this effect and in 2004 the cloud fraction in low and mid-levels is somewhat underestimated. The model's recent tendency towards an underestimation of low level cloud was previously indirectly confirmed by long term comparisons of the operational model to synoptic surface observations of total cloud cover. However, the lack of vertical structure information in these observations prevented the correction of the bias. This emphasises the importance of the Cloudnet goal of providing quasi-realtime feedback to the model developers. Had this information concerning vertical structure of the biases at these European stations been available at the time of these model developments in the pre-2004 period, then it is more likely that they could have been effectively tackled prior to operational implementation. This demonstrates that the Cloudnet database also provides a valuable source for climate modelling groups when evaluating cloud statistics and for testing new cloud parameterizations.

4. Evaluation of model water content

The Atmospheric Model Intercomparison Project (AMIP) has highlighted the worrying order-of-magnitude spread in mean cloud water content between different climate models (Stephens *et al.*, 2002), despite them all being constrained by observed top-of-atmosphere fluxes. In addition to cloud fraction, the Cloudnet observations have been used to evaluate liquid water content (LWC) and ice water content (IWC) in the models. The LWC profile can be estimated directly from radar and lidar measurements (Krasnov and Russchenberg, 2005) or, alternatively, from the integrated LWP if the cloud thickness is known by assuming that the value of LWC increases linearly with height from zero at cloud base (Albrecht *et al.* 1990, Boers *et al.* 2000). The location of liquid cloud is taken from the categorization data, essentially with the lidar providing cloud base and radar providing cloud top height. The profile of LWC is scaled so that the integral matches the LWP derived from the dual-wavelength microwave radiometers. The error in the long-term mean LWC due to this simple partitioning of LWC with height is easily gauged by comparing with a retrieval assuming a top-hat LWC profile within each layer. In practice, most liquid water clouds are thin, occupying only a few vertical model levels, so the effect on mean LWC is small and this method is adequate for evaluating models.

Figure 7 shows the performance of LWC in the seven models over all three sites during 2004, including errors. Periods when rain was measured at the surface have been excluded from the comparisons. Below 2km the Met Office and ECMWF generally agree closest with the LWC observations in the mean, while a number of errors are evident in the other models; RCA tending to overestimate the mean LWC (as it does with cloud fraction) while both DWD and Météo-France have too little LWC. The PDFs in Fig. 7b show that Météo-France (which diagnoses water content from humidity) tends to have too narrow a distribution of LWC. For the prognostic LWC in the other models, ECMWF tends to overestimate the occurrence of liquid water cloud but underestimate the water content when it is present, and for DWD the absence of high LWC in the PDF explains the low mean values of LWC in Figure 7a. The RACMO model largely shares its cloud scheme with ECMWF, and consequently its LWC errors are rather similar. It should be stressed that low LWC values can still have a significant radiative impact so it is important that the PDF is represented well, not just the long-term mean.

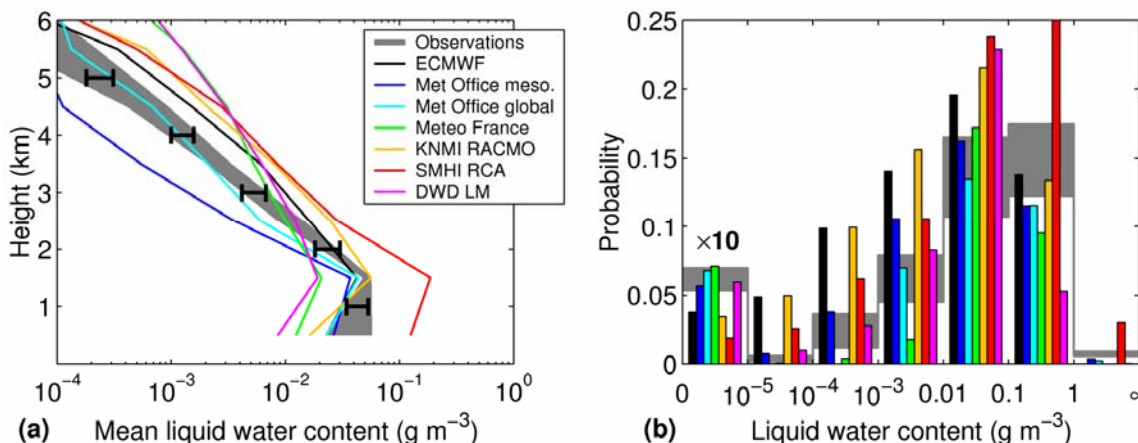


Figure 7. (a) Mean liquid water content over three sites for 2004 observations and the seven models (for further details see Figure 3). Errors in the observations are due to the assumed vertical distribution of LWC within the cloud, and any error in the radiometer LWP. The error bars were calculated by comparing LWC derived assuming a triangular and a top-hat LWC distribution within each layer; the effect of an additional 10% error in LWP was also included. Note that in the presence of multiple layers, the phase discrimination can be problematic because the lidar fails to penetrate the lowest layer, hence LWC above 2 km is less reliable, and it is difficult to quantify the models' ability to represent supercooled clouds. (b) Histograms of LWC for clouds between 0 and 3 km altitude.

In Cloudnet, three techniques have been developed to retrieve IWC, supplementing the radar reflectivity by either lidar backscatter (Donovan *et al.* 2001, Donovan, 2003; Tinel *et al.*, 2005), Doppler velocity (Matrosov *et al.*, 1995; the radar-only “RadOn” method of Delanoë *et al.*, 2007) or model temperature (Liu and Illingworth 2000, Hogan *et al.*, 2006a). While the radar-lidar method is expected to be the most accurate (Hogan *et al.*, 2006b), extinction of the lidar signal means that it is only applicable to around 10% of the ice clouds over the Cloudnet sites. Instantaneous errors in the reflectivity-temperature method are estimated to be about a factor of two below -40°C , reducing to about 50% for temperatures above -20°C (Hogan *et al.* 2006a). Comparisons between the methods indicate that, while there is a substantial degree of scatter in individual cases, for the higher values of IWC they report approximately the same long-term mean values, so to ensure a large dataset with which to evaluate the models we use the reflectivity-temperature method of Hogan *et al.* (2006a) in the remainder of the paper. Care has been taken to ensure that periods with rain at the surface have been excluded from the analysis, as on such occasions the radar tends to be significantly attenuated by the melting layer, the rain drops and a layer of water on the radar itself. Hence the comparisons that follow are predominantly of non-precipitating ice clouds, but note that the radar-temperature method has previously been applied to precipitating ice clouds using a longer wavelength radar (Hogan *et al.*, 2006a). The probability distribution function (PDF) of IWC within a grid-box could be used to evaluate future cloud schemes based on sub-grid scale variability (e.g. Tompkins 2002, Hogan and Illingworth 2003) but here we consider only grid-box mean IWC values.

Figure 8 compares the performance of IWC forecasts in the seven models against observations at the three sites during 2004, including errors. It can be seen that the Met Office mesoscale and ECMWF models reproduce the mean IWC within the uncertainty of the IWC retrieval. Below 0.1 g m^{-3} the DWD model has the best representation of the PDF, but because it treats falling snow as a separate non-cloud variable it predicts virtually no IWC above this, thus the mean IWC below 7 km is substantially underestimated. If falling snow were included as cloud it might improve the IWC comparison, but would worsen the cloud fraction comparison. As with LWC, the Météo-France model mean value of IWC is too low, mainly because it is simulating too narrow a distribution of IWC; this PDF behavior is shared by the Met Office global model but less so by the mesoscale version. Subdividing the data into seasons confirmed that similar behavior in the models is observed in all seasons. Full monthly and yearly plots for the radar-temperature method are available on the Cloudnet web site.

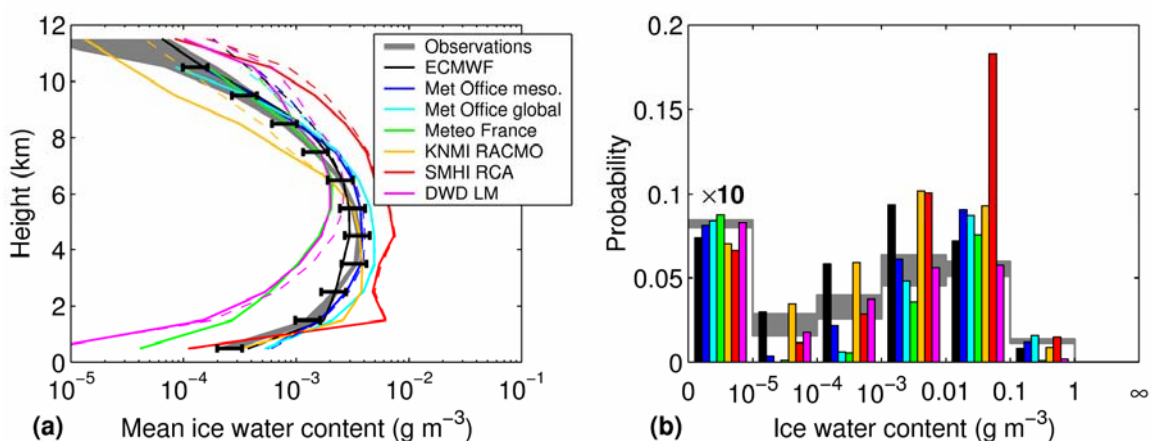


Figure 8. As Fig. 7 but for ice water content. The histogram in (b) is for clouds between 3 and 7 km. As in Fig. 3, model values are shown both before and after filtering. The error bars were calculated by changing the minimum-detectable radar reflectivity by $\pm 3\text{ dB}$, but with an additional 25% error to represent a possible systematic 1-dB radar calibration error at all sites (resulting in a 15% error in mean IWC), and a possible 20% uncertainty in the mass-diameter relationship.

5. Evaluation of model drizzle rates

At the base of stratocumulus clouds, the combination of the radar to lidar may be used to estimate the parameters of the drizzle size distribution (number concentration, median drop size and drop spectrum shape), and hence the drizzle liquid water flux, using the method of O'Connor *et al.* (2005). Drizzle rates are crucially important in climate models due to their impact on cloud evolution and lifetime, because drizzle evaporation affects the thermodynamic structure, and if the drizzle reaches the surface then it represents a sink of moisture from the boundary layer. Drizzle rates have been derived from a year of data at Chilbolton and compared to the values in several of the models in Cloudnet. Rather than perform a point-by-point comparison of drizzle, which would be very noisy, the grey points in Fig. 9 show the observed drizzle rates at cloud base (assumed to be the maximum rate in the profile) as a function of the cloud liquid water path (LWP, derived from microwave radiometers). The target classification (Fig. 2) is used to isolate precipitation originating from the warm rain process rather than melting ice. The black points in Fig. 9 show the corresponding values for the ECMWF and Met Office mesoscale models, again isolating precipitation associated with the warm rain process. It is clear that, while the models have a similar distribution of LWP, the drizzle rate for a given value of LWP tends to be substantially overestimated. Similar results are obtained from the Met Office global model and the Météo-France model (O'Connor *et al.*, 2007).

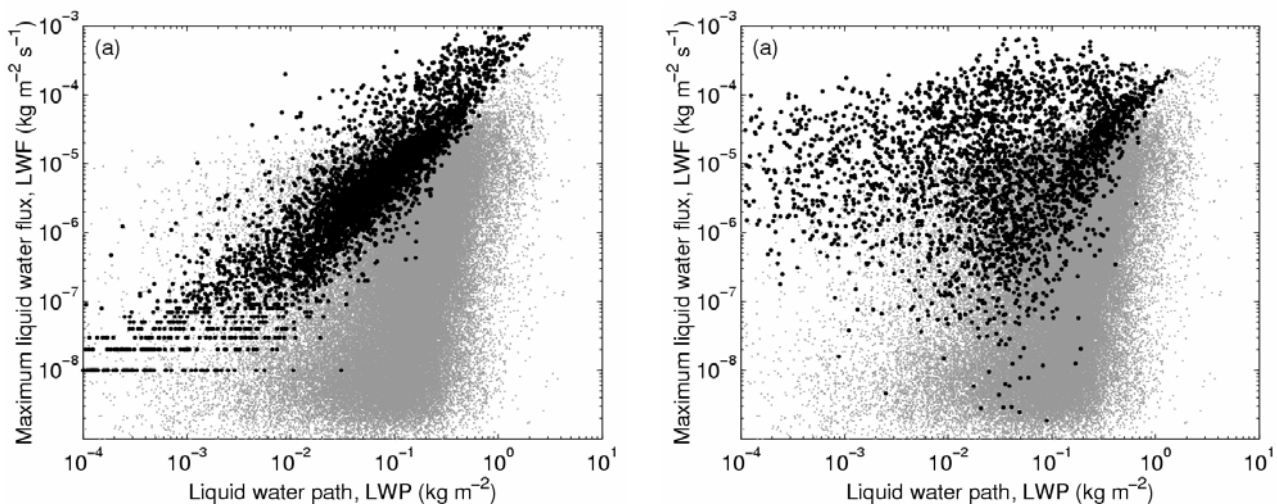


Figure 9. Scatterplots of cloud liquid water path versus the maximum drizzle liquid water flux in the profile, for the 12 months April 2003 to March 2004 at Chilbolton. The ECMWF model values are shown by the black points on the left panel and the Met Office mesoscale model by the black points on the right panel. The observations (at 30-s resolution) are shown by the grey points.

There are a number of possible causes of the incorrect drizzle rate, the most likely candidates being a too-high auto-conversion rate or an error in the assumed drizzle size distribution leading to an incorrect rate of accretion of liquid water droplets. The latter is difficult to assess for models such as ECMWF, in which the drizzle size distribution is entirely implicit, but for the Met Office there is a one-to-one relationship between the mean drizzle drop size and the drizzle rate. O'Connor *et al.* (2007) have shown that the mean drop size in the Met Office relationship is too large for a given drizzle rate, resulting in the drops falling too fast and evaporating too slowly. This explains the finding that drizzle in the models is far more likely to reach the ground than in the observations. There is a clear need for warm rain parametrization schemes to be modified based on observations such as these.

6. Cloud fraction skill scores

The comparisons so far have evaluated the *climatology* of the model, not the quality of the specific *forecast*. For this we use skill scores. Firstly the observed and modelled cloud fraction values are converted to binary fields using a threshold cloud fraction value. Then a contingency table is constructed, containing the number of times cloud occurred both in observations and model (A), the times cloud occurred neither in the observations nor the model (D), and the times that it occurred in the model or the observations but not both (B and C). Numerous skill scores can be calculated from the values A – D but to be useful they should ideally have the properties that they are independent of the frequency of occurrence of the event, and that a random forecast should produce a score of zero. Most simple scores such as hit rate and false alarm rate (e.g. Mace *et al.*, 1998) have neither of these properties, so we have used the Equitable Threat Score (ETS), which has been found to vary only weakly with cloud fraction threshold, and produces 0 for a random forecast and 1 for a perfect forecast. It is defined as $ETS=(A-E)/(A+B+C-E)$, where E is the number of hits that occurred by chance, given by $E=(A+B)(A+C)/(A+B+C+D)$.

Figure 10 shows the evolution of ETS at Cabauw for Cloudnet observations from August 2001 to June 2005, using a threshold cloud fraction of 0.05. To put these numbers in context, also shown is the score obtained for a “persistence” forecast. There is distinct evidence for more skillful forecasts in winter than summer, presumably due to the greater difficulty in representing convective than stratiform systems, but it is noticeable that the seasonal variation is larger than the very weak long-term trend for increasing skill over time. Furthermore, with a threshold of 0.05 there is no evidence of a sudden change in Météo-France skill in April 2003 as might be expected from Figs. 4 and 5. The reason is that this measure of skill is more dependent on the representation of large-scale moisture and the quality of the data assimilation, rather than the subtleties of the cloud scheme. RCA is run without data assimilation in climate mode over a large area which partly explains the lower forecast skill.

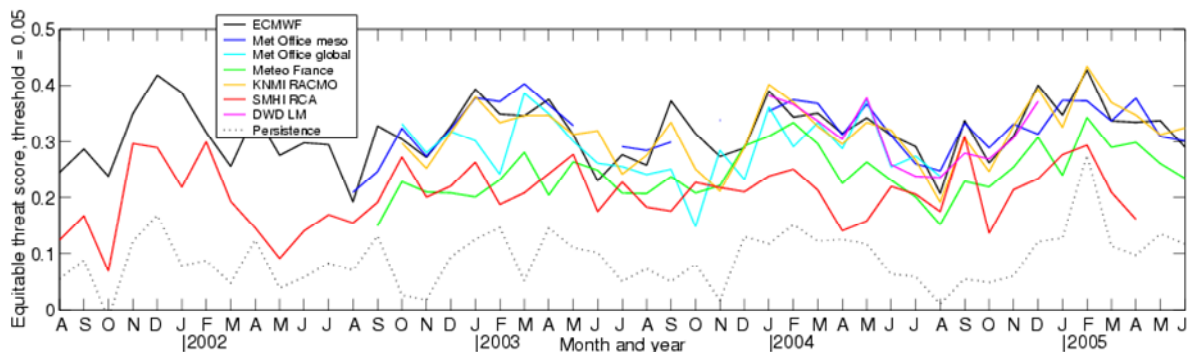


Figure 10. Equitable threat score for forecasts of cloud fraction greater than 0.05, versus time, for the seven models at the Cabauw site (which has the longest time series of observations of the three sites). Also shown is the skill of the persistence forecast, which consists of using the observed cloud fraction 24 hours previously as a function of height as the forecast. Note that the lead-time for most of the models is around 24 hours.

7. Conclusions

The Cloudnet project has shown that continuous profiles of cloud fraction, liquid water content and ice water content can be inferred reliably from a simple set of ground based instruments comprising a cloud radar, a lidar ceilometer and microwave radiometers, and that these profiles can then be systematically compared with the representation of the clouds in operational forecast models. Additional work as part of Cloudnet, not documented here, has explored the retrieval of turbulent dissipation rate in clouds using Doppler radar (Bouniol *et al.*, 2003), the occurrence of cirrus clouds that are too optically thin to be detected by radar but can be seen with high-power lidar (Morille *et al.*, 2006; Cadet *et al.*, 2005; Noel *et al.*, 2005), a

parameterization of ice effective radius based on distance below cloud-top from combined radar and lidar observations (van Zadelhoff *et al.*, 2004) and the retrieval of cloud inhomogeneity from radar (Hogan and Illingworth, 2003). Work is in progress to develop a “unified” cloud retrieval scheme in which radar, lidar and radiometer observations would be combined in a variational framework to find the optimum profile of cloud microphysics that correctly forward-models all the observations.

With a little further development it will be possible to apply the Cloudnet algorithms in near realtime, providing rapid feedback on the model performance and allowing the impact of changes to cloud schemes to be tested prior to their operational implementation. The findings reported in this paper are confined to sites in North West Europe. Following a decision of the Global Energy and Water Cycle Experiment (GEWEX) Working Group on Cloud and Aerosol Profiling in 2004 the analysis is being extended to Lindenberg (Germany) and the ARM sites in Oklahoma, the North Slope of Alaska, and the three stations in the Tropical Western Pacific. The first results of these comparisons can be viewed at the Cloudnet web site: <http://www.cloud-net.org/>. The Cloudnet analysis could be easily extended to additional observing sites in different geographical locations and only simple changes are needed to incorporate additional forecasting models. We would welcome approaches from researchers wishing to engage in such a collaboration.

Acknowledgements. The Cloudnet project was funded by the European Union from grant EVK2-2000-00065. The Cabauw Experimental Site for Atmospheric Research, or CESAR Observatory, results from a consortium agreement lead by the Dutch weather services KNMI. The Chilbolton Facility for Atmospheric and Radio Research (CFARR) is funded largely through the UK Natural Environment Research Council (NERC). The SIRTa (Site Instrumental de Recherche par Télédétection Atmosphérique) Observatory in Palaiseau was established by the Institut Pierre Simon Laplace and is supported by CNRS, CNES (the French Space Agency) and Ecole Polytechnique.

8. References

- Ibrecht, B. A., C. W. Fairall, D. W. Thomson, A. B. White, J. B. Snider, W. H. Schubert, 1990: Surface-based remote-sensing of the observed and the adiabatic liquid water-content of stratocumulus clouds, *Geophys. Res. Lett.*, **17**, 89-92.
- Boers, R., H. Russchenberg, J. Erkelens, V. Venema, A. van Lammeren, A. Apituley and S. J. Jongen, 2000: Ground-based remote sensing of stratocumulus properties during CLARA, 1996, *J. Appl. Meteorol.*, **39**, 169-181.
- Bouniol, D., A. J. Illingworth and R. J. Hogan, 2003: Deriving turbulent kinetic energy dissipation rate within clouds using ground based 94 GHz radar, *Proc. 31st AMS Conf. on Radar Meteorology, Seattle*, 192-196.
- Brooks, M. E., R. J. Hogan and A. J. Illingworth, 2005: Parameterizing the difference in cloud fraction defined by area and by volume as observed with radar and lidar. *J. Atmos. Sci.*, **62**, 2248-2260.
- Cadet B., V. Giraud, M. Haeffelin, P. Keckhut, A. Rehou and S. Baldy, 2005: Improved retrievals of cirrus cloud optical properties using a combination of lidar methods, *Applied Optics*, **44**, 1726-1734.
- Crewell, S., C. Simmer, H. Bloemink, A. Feijt, S. García, D. Jolivet, O. Krasnov, A. van Lammeren, U. Löhnert, E. van Meijgaard, J. Meywerk, K. Pfeilsticker, M. Quante, S. Schmidt, M. Schröder, T. Scholl, T. Trautmann, V. Venema, M. Wendisch, U. Willén, 2004: The BALTEX Bridge Campaign: An integrated approach for a better understanding of clouds, *Bull. Amer. Meteor. Soc.*, **85**, 1565-1584, doi: 10.1175/BAMS-85-10-1565.

- Delanoë, J., A. Protat, D. Bouniol, J. Testud, A. Heymsfield, A. Bansemmer and P. Brown, 2007: RadOn; a new method for retrieval of the dynamical, microphysical and radiative properties of ice clouds from Doppler cloud radar observations. *J. Appl. Meteorol.*, submitted.
- Doms, G., J. Foerstner, E. Heise, H.-J. Herzog, M. Raschendorfer, R. Schrodin, T. Reinhardt and G. Vogel, 2004: A description of the nonhydrostatic regional model LM. 2 – Physical parameterization. Deutscher Wetterdienst technical report.
- Donovan, D. P., 2003: Ice-cloud effective particle size parameterization based on combined lidar, radar reflectivity, and mean Doppler velocity measurements, *J. Geophys. Res.*, **108**, 4573, doi:10.1029/2003JD003469.
- Donovan, D. P., A.C.A.P. van Lammeren, R. J. Hogan, H. W. J. Russchenberg, A. Apituley, P. Francis, J. Testud, J. Pelon, M. Quante and J. W. F. Goddard, 2001: Cloud effective particle size and water content profile retrievals using combined lidar and radar observations - 2. Comparison with IR radiometer and in situ measurements of ice clouds, *J. Geophys. Res.*, **106**, 27449-27464.
- Ducrocq, V., and P. Bougeault, 1995: Simulations of an observed squall line with a meso-beta scale hydrostatic model, *Wea. Forecasting*, **10**, 380-399.
- Gaussiat, N., R. J. Hogan, and A. J. Illingworth, 2007: Accurate liquid water path retrieval from low-cost microwave radiometers using additional information from a lidar ceilometer and operational forecast models. Accepted *J. Atmos. Oceanic. Technol.*
- Goddard, J. W. F., J. Tan and M. Thurai, 1994: Technique for calibration of meteorological radars using differential phase, *Elect. Lett.*, **30**, 166-167.
- Greenwald, T. J., G. L. Stephens, T. H. Vonder Haar and D. L. Jackson, 1993: A physical retrieval of cloud liquid water over the global oceans using special sensor microwave/imager (SSM/I) observations, *J. Geophys. Res.*, **98**, 18471-18488.
- Haeffelin, M., L. Barthès, O. Bock, C. Boitel, S. Bony, D. Bouniol, H. Chepfer, M. Chiriaco, J. Cuesta, J. Delanoë, P. Drobinski, J.-L. Dufresne, C. Flamant, M. Grall, A. Hodzic, F. Hourdin, F. Lapouge, Y. Lemaître, A. Mathieu, Y. Morille, C. Naud, V. Noël, B. O'Hirok, J. Pelon, C. Pietras, A. Protat, B. Romand, G. Scialom, R. Vautard, 2005: SIRTa, a ground-based atmospheric observatory for cloud and aerosol research. *Annales Geophysicae*, **23**, 253-275.
- Hogan, R. J., and A. J. Illingworth, 2000: Deriving cloud overlap statistics from radar. *Q. J. R. Meteorol. Soc.*, **126**, 2903-2909.
- Hogan, R. J., C. Jakob and A. J. Illingworth, 2001: Comparison of ECMWF winter-season cloud fraction with radar-derived values, *J. Appl. Meteorol.*, **40**, 513-525.
- Hogan, R. J., and A. J. Illingworth, 2003: Parameterizing ice cloud inhomogeneity and the overlap of inhomogeneities using cloud radar data. *J. Atmos. Sci.*, **60**, 756-767.
- Hogan, R. J., and E. J. O'Connor, 2004: Facilitating cloud radar and lidar algorithms: the Cloudnet Instrument Synergy/Target Categorization product. Cloudnet documentation: <http://www.cloudnet.org/data/products/categorize.html>.
- Hogan, R. J., D. Bouniol, D. N Ladd, E. J. O'Connor and A. J. Illingworth, 2003a: Absolute calibration of 94/95-GHz radars using rain, *J. Atmos. Oceanic. Technol.*, **20**, 572-580.
- Hogan, R. J., A. J. Illingworth, E. J. O'Connor and J. P. V. Póiares Baptista, 2003b: Characteristics of mixed-phase clouds: Part II: A climatology from ground-based lidar, *Quart. J. Roy. Meteorol. Soc.*, **129**, 2117-2134.

- Hogan, R. J., M. P. Mittermaier and A. J. Illingworth, 2006a: The retrieval of ice water content from radar reflectivity factor and temperature and its use in evaluating a mesoscale model. *J. Appl. Meteorol.*, **45**, 301-317.
- Hogan, R. J., D. P. Donovan, C. Tinel, M. A. Brooks, A. J. Illingworth and J. P. V. Poyares Baptista, 2006b: Independent evaluation of the ability of spaceborne radar and lidar to retrieve the microphysical and radiative properties of ice clouds, *J. Atmos. Oceanic. Technol.*, **23**, 211-227.
- Illingworth, A. J., R. J. Hogan, E. J. O'Connor, D. Bouniol, M. E. Brooks, J. Delanoe, D. P. Donovan, N. Gaussiat, J. W. F. Goddard, M. Haeffelin, H. Klein Baltink, O. A. Krasnov, J. Pelon, J.-M. Piriou, A. Protat, H. W. J. Russchenberg, A. Seifert, A. M. Tompkins, G.-J. van Zadelhoff, F. Vinit, U. Willen, D. R. Wilson and C. L. Wrench, 2007: Cloudnet - continuous evaluation of cloud profiles in seven operational models using ground-based observations. *Bull. Am. Meteorol. Soc.*, in press.
- Jakob, C., 2003; An improved strategy for the evaluation of cloud parameterizations in GCMs, *Bull. Am. Meteorol. Soc.*, **84**, 1387-1401.
- Korolev, A., G.A. Isaac and J. Hallet, 2000: Ice particle habits in stratiform clouds. *Quart. J. Roy. Meteorol. Soc.*, **126**, 2873-2902.
- Krasnov, O. A. and H. W. J. Russchenberg, 2005: A synergetic radar-lidar technique for the LWC retrieval in water clouds description and application to CLOUDNET data, *11th conference on Mesoscale processes and the 32nd conference on Radar Meteorology*, Albuquerque, New Mexico.
- Li, J.-L., D. E. Waliser, J. H. Jiang, D. L. Wu, W. Read, J. W. Waters, A. M. Tompkins, L. J. Donner, J.-D. Chern, W. -K. Tao, R. Atlas, Y. Gu, K. N. Liou, A. Del Genio, M. Khairoutdinov and A. Gettelman, 2005: Comparisons of EOS MLS cloud ice measurements with ECMWF analyses and GCM simulations: Initial results, *Geophys. Res. Lett.*, **32**, L18710, doi:10.1029/2005GL023788.
- Liu, C.-L., and A. J. Illingworth, 2000: Towards more accurate retrievals of ice water content from radar measurements of clouds, *J. Appl. Meteorol.*, **39**, 1130-1146.
- Mace, G. G., and S. Benson-Troth, 2002: Cloud-layer overlap characteristics derived from long-term cloud radar data. *J. Climate*, **15**, 2505-2515.
- Mace, G. G, C. Jakob and K. P. Moran, 1998: Validation of hydrometeor occurrence predicted by the ECMWF model using millimeter wave radar data, *Geophys. Res. Lett.*, **25**, 1645-1648.
- Matrosov, S. Y. ,A. J. Heymsfield, J. M. Intrieri, B. W. Orr and J. B. Snider, 1995: Ground-Based Remote Sensing of Cloud Particle Sizes during the 26 November 1991 FIRE II Cirrus Case: Comparisons with In Situ Data, *J. Atmos. Sci.*, **52**, 4128-4142.
- Morille Y., M. Haeffelin, P. Drobinski and J. Pelon, 2006: STRAT: An algorithm to retrieve the STRucture of the ATmosphere from single channel lidar data, *J. Atmos. Ocean. Technol.*, submitted.
- Noel V., D. M. Winker, M. Haeffelin, M. McGill, 2006: Comparison of depolarization ratios observed in convective ice clouds during CRYSTAL-FACE with a midlatitude synoptic cirrus clouds climatology from the SIRTa observatory, *J. Geophys. Res.*, submitted.
- O'Connor, E. J., A. J. Illingworth and R. J. Hogan, 2004: A technique for autocalibration of cloud lidar, *J. Atmos. Oceanic. Technol.*, **21**, 777-786.
- O'Connor, E. J., R. J. Hogan and A. J. Illingworth, 2005: Retrieving stratocumulus drizzle parameters using Doppler radar and lidar, *J. Appl. Meteorol.*, **44**, 14-27.

- O'Connor, E. J., R. J. Hogan, A. J. Illingworth and C. D. Westbrook, 2007: How do model parameterizations of drizzle compare to radar and lidar observations? *Submitted to J. Climate*.
- Protat A., A. Armstrong, M. Haeffelin, Y. Morille, J. Pelon, J. Delanoë, and D. Bouniol, 2006: The impact of conditional sampling and instrumental limitations on the statistics of cloud properties derived from cloud radar and lidar at SIRTa, *Geophys. Res. Lett.*, in press.
- Rasch, P.J., and J. E. Kristjánsson, 1998: A comparison of the CCM3 model climate using diagnosed and predicted condensate parameterizations, *J. Clim.*, **11**, 1587-1614.
- Ricard, J. L., and J. F. Royer, 1993: A statistical cloud scheme for use in an AGCM. *Annales Geophysicae*, **11**, 1095-1115.
- Rossow, W. B. and R. A. Schiffer, 1991: ISCCP Cloud Data Products. *Bull. Amer. Meteor. Soc.*, **72**, 2-20.
- Smith, R. N. B., 1990: A scheme for predicting layer clouds and their water content in a general circulation model. *Quart. J. Roy. Meteorol. Soc.*, **116**, 435-460.
- Stephens, G. L., D. G. Vane, R. Boain, G. G. Mace, K. Sassen, Z. Wang, A. J. Illingworth, E. J. O'Connor, W. Rossow, S. L. Durden, S. D. Miller, R. T. Austin, A. Benedetti, C. Mitrescu, 2002: The CloudSat mission and the A-Train. *Bull. Am. Meteorol. Soc.*, **83**, 1771-1790.
- Stokes, G. M. and S. E. Schwartz, 1994: The Atmospheric Radiation Measurement (ARM) Program: Programmatic Background and Design of the Cloud and Radiation Test Bed, *Bull. Amer. Meteor. Soc.*, **75**, 1201-1221.
- Tiedtke, M., 1993: Representation of clouds in large-scale models. *Mon. Weath. Rev.*, **121**, 3040-3061.
- Tinel, C., J. Testud, R. J. Hogan, A. Protat, J. Delanoë and D. Bouniol, 2005: The retrieval of ice cloud properties from cloud radar and lidar synergy. *J. Appl. Meteorol.*, **44**, 860-875.
- Tompkins, A. M., 2002: A prognostic parameterization for the subgrid-scale variability of water vapour and clouds in large-scale models and its use to diagnose cloud cover. *J. Atmos. Sci.*, **59**, 1917-1942.
- van Meijgaard, E. and S. Crewell, 2005: Comparison of model predicted liquid water path with ground-based measurements during CLIWA-NET, *Atmos. Res.*, **75**, 201-226.
- van Zadelhoff, G.-J., D. P. Donovan, H. Klein Baltink and R. Boers, 2004: Comparing ice cloud microphysical properties using CloudNET and Atmospheric Radiation Measurement Program data, *J. Geophys. Res.*, **109**, D24214, doi:10.1029/2004JD004967.
- Webb, M., C. Senior, S. Bony and J.-J. Morcrette, 2001: Combining ERBE and ISCCP data to assess clouds in the Hadley Centre, ECMWF and LMD atmospheric climate models, *Climate Dynamics*, **17**, 905-922.
- Willén U., S. Crewell, H. Klein Baltink and O. Sievers 2005: Assessing model predicted vertical cloud structure and cloud overlap with radar and lidar ceilometer observations for the Baltex Bridge Campaign of CLIWA-NET, *Atmos. Res.*, **75**, 227-255.
- Wilson, D. R. and S. P. Ballard, 1999: A microphysically based precipitation scheme for the Meteorological Office Unified Model. *Q. J. R. Meteorol. Soc.*, **125**, 1607-1636.
- Winker, D. M., J. Pelon, and M. P. McCormick, 2003; The CALIPSO mission: spaceborne lidar for observation of aerosols and clouds. *Proc of SPIE*, **4893**, 1-11.
- Xu, K.-M., and D. A. Randall, 1996: A semiempirical cloudiness parameterization for use in climate models, *J. Atmos. Sci.*, **53**, 3084-3102.